Published online 2 May 2017

Nucleic Acids Research, 2017, Vol. 45, No. 10 ***5995–6010***
doi: 10.1093/nar/gkx325

Roles of the C-terminal domains of topoisomerase IIα and topoisomerase IIβ in regulation of the decatenation checkpoint

Toshiyuki Kozuki[1,†], Kenichi Chikamori[1,†], Marius D. Surleac[2,†], Marius A. Micluta[2], Andrei J. Petrescu[2], Eric J. Norris[3], Paul Elson[1], Gerald A. Hoeltge[4], Dale R. Grabowski[1], Andrew C.G. Porter[5], Ram N. Ganapathi[3,*] and Mahrukh K. Ganapathi[3,*]

[1]Taussig Cancer Institute, Cleveland Clinic, 9500 Euclid Avenue, Cleveland, OH 44195, USA, [2]Department of Bioinformatics, Institute of Biochemistry of the Romanian Academy, Bucharest, Romania, [3]Department of Cancer Pharmacology, Levine Cancer Institute, Carolinas HealthCare System, 1021 Morehead Medical Drive, Charlotte, NC 28204, USA, [4]Clinical Pathology, Cleveland Clinic, 9500 Euclid Avenue, Cleveland, OH 44195, USA and [5]Imperial College Faculty of Medicine, Hammersmith Hospital, London W10 ONN, UK

Received December 02, 2016; Revised April 11, 2017; Editorial Decision April 13, 2017; Accepted April 14, 2017

ABSTRACT

Topoisomerase (topo) IIα and IIβ maintain genome stability and are targets for anti-tumor drugs. In this study, we demonstrate that the decatenation checkpoint is regulated, not only by topo IIα, as previously reported, but also by topo IIβ. The decatenation checkpoint is most efficient when both isoforms are present. Regulation of this checkpoint and sensitivity to topo II-targeted drugs is influenced by the C-terminal domain (CTD) of the topo II isoforms and by a conserved non-catalytic tyrosine, Y640 in topo IIα and Y656 in topo IIβ. Deletion of most of the CTD of topo IIα, while preserving the nuclear localization signal (NLS), enhances the decatenation checkpoint and sensitivity to topo II-targeted drugs. In contrast, deletion of most of the CTD of topo IIβ, while preserving the NLS, and mutation of Y640 in topo IIα and Y656 in topo IIβ inhibits these activities. Structural studies suggest that the differential impact of the CTD on topo IIα and topo IIβ function may be due to differences in CTD charge distribution and differential alignment of the CTD with reference to transport DNA. Together these results suggest that topo IIα and topo IIβ cooperate to maintain genome stability, which may be distinctly modulated by their CTDs.

INTRODUCTION

Topoisomerase (topo) II alters DNA topology by resolving supercoils and catenations in chromosomal DNA (1–3). This enzyme plays a vital role in DNA metabolic processes, including chromosome condensation and segregation and transcription. In vertebrates two isoforms of topo II, topo IIα and topo IIβ, are present. These isoforms are structurally similar in the N-terminal ATP binding domain and the DNA binding catalytic domain (1–3). However, the C-terminal domains of topo IIα and topo IIβ exhibit only 22% identity. Although topo IIα and topo IIβ display similar catalytic activities they exhibit distinct functional activities, which in part may be due to the structural diversity of the C-terminal domain (CTD). Extensive studies of the topo IIα isoform have shown that it is expressed in proliferating cells during the S and G2M phases of the cell cycle and is primarily involved in regulating cell proliferation (1–5). However, the topo IIβ isoform, which is constitutively expressed (4,5), is mainly associated with cell differentiation (6–9) and transcription (10,11). Studies in topo IIβ knockout mice support a role for this isoform in neuronal development (12).

The decatenation activity of topo II is essential for separating the entangled sister chromatids that form during DNA replication. The efficient removal of the catenae is required for proper chromosome condensation in prophase and chromosome segregation in anaphase. Consequently, perturbation of topo II activity prevents decatenation and disentanglement of the chromosomes and leads to activa-

*To whom correspondence should be addressed. Tel: +1 704 355 9762; Fax: +1 704 446 7519: Email: mahrukh.ganapathi@carolinashealthcare.org
Correspondence may also be addressed to Ram N. Ganapathi. Tel: +1 704 355 9759; Email: ram.ganapathi@carolinashealthcare.org
†These authors contributed equally to the work as first authors.
Present addresses:
Toshiyuki Kozuki, Shikoku Cancer Center, 160 Kou Minamiumemoto cho, Matsuyama, Ehime 791-0280, Japan.
Kenichi Chikamori, Yamaguchi-Ube Medical Center, 685 Higashi-kiwa, Ube, Yamaguchi 755-0241, Japan.

tion of the decatenation checkpoint, which delays progression of G2 cells into mitosis (13–15). Activation of this checkpoint, which is distinct from the DNA damage checkpoint (16), is essential for maintaining cellular integrity and genome stability. Thus a defective checkpoint could lead to genome instability, aneuploidy and development of cancer. Although the mechanism by which cells activate the decatenation checkpoint is not fully understood, it has been suggested that a chromatin structural feature probably involving the presence of a topo II dimer in association with catenated DNA serves as a sensor for activating this checkpoint (17). Studies evaluating the decatenation checkpoint using topo II catalytic inhibitors, such as the bisdioxopiperazine, ICRF-193 to perturb topo II activity have suggested that topo IIα is the main isoform involved in regulating this checkpoint (18–20). Given the almost identical catalytic activities of topo IIα and topo IIβ and the essential nature of topo II activity in maintaining cellular integrity, these isoforms could exhibit overlapping functional activities. The topo II isoforms may be uniquely regulated by interactions with protein complexes, post-translational modifications (PTMs) or by localizations to specific regions within the nucleus (21). For such regulation the divergent CTD likely plays an important role. In this study, we examined the role of both isoforms in regulating the decatenation checkpoint and evaluated the influence of deleting the CTD as well as mutating a conserved non-catalytic tyrosine that was previously shown to alter the in vitro catalytic activity of topo IIβ (22). Further, the sensitivity of wild type (WT) and mutant forms of topo IIα and topo IIβ to topo II-targeted drugs was also studied

MATERIALS AND METHODS

Reagents

Polyclonal antibodies for topo IIα and topo IIβ have been described previously (22,23). The antibody to myc-tag protein (clone A46) was obtained from EMD Millipore (Billerica, MA). Anti-β-actin-peroxidase antibody (clone AC-15) was purchased from Sigma-Aldrich (St. Louis, MO, USA). Geneticin and puromycin were obtained from Life Technologies (Carlsbad, CA, USA). Tetracycline (Tet) was obtained from Sigma-Aldrich (St. Louis, MO, USA). The topo II catalytic inhibitor ICRF-193 was obtained from MP Biomedicals (Santa Ana, CA, USA). The topo II-targeting drugs etoposide (VP-16) and amsacrine (*m*-AMSA) were obtained from Sigma-Aldrich (St. Louis, MO) and the NCI, NIH, respectively. Stock solutions of these drugs were prepared in dimethyl sulfoxide (Sigma-Aldrich, St. Louis, MO) and stored at –20°C. Karyomax® colcemid solution was obtained from Life Technologies (Carlsbad, CA, USA). Muse H2A.X activation dual detection kit was obtained from EMD Millipore (Billerica, MA, USA). Vectashield mounting medium for fluorescence with DAPI was purchased from Vector Laboratories Inc. (Burlingame, CA, USA). *Kinetoplast* DNA (*k*DNA) was obtained from Topogen (Columbus, OH, USA).

Construction of human WT and mutant topo IIα and topo IIβ cDNA plasmids

WT topo IIα and topo IIβ (topo IIβ sequence based on isoform 1 comprising of 1621 amino acids—NCBI accession NP_001059) cDNAs contained a c-Myc and 6xHis linker at the 3′ end. C-terminal deleted (C-del) topo IIα corresponding to deletion of K1201-Q1453 and F1498-F1531 and C-del topo IIβ corresponding to deletion of K1219-S1521 and Q1574-N1621, were constructed by site-directed mutagenesis of the WT cDNA using the Quick-change site-directed mutagenesis kit (Agilent Technologies, Inc., Santa Clara, CA, USA). In both C-del constructs the nuclear localization signals (K1454-D1497 for topo IIα and E1522-R1573 for topo IIβ) were preserved (24). The primer set for topo IIα K1201-Q1453 deletion was 5′-AAG CCT GAT CCT GCC AAA ACC AAG AAT CG-3′ and 5′-GG CCT TCC CCC CTT TCC CAG -3′, whereas the primer set for topo IIα -D1498-F1531 deletion was 5′- GAA CAA AAG TTG ATC TCT GAA GAA GAC TTG AAC-3′ and 5′-GTC ATC ACT CTC CCC CTT GG-3′. The primer set for topo IIβ K1219-S1521 deletion was 5′-AGG TTT GCC AAC TTT ACC TTT AAT TG-3′ and 5′-GAA TTT GGC ATT CCA AAG AAG ACT ACA AC-3′, whereas the primer set for topo IIβ Q1574-N1621 deletion was 5′-ATC AAA AGA TGT CTT CTT CGG TTT CTT GC-3′ and 5′-GAA CAA AAG TTG ATC TCT GAA GAA GAC TTG AAC-3′. The Y640F mutant topo IIα and Y656F mutant topo IIβ cDNA were also constructed by site-directed mutagenesis. The primer set used for generating the Y640F mutant topo IIα was, 5′-CAT CGT ATC CAG TTC AAA TTT TCT GGT CCT GAA GAT GAT GCT GC-3′ and 5′-GC AGC ATC ATC TTC AGG ACC AGA AAA TTT GAA CTG GAT ACG ATG-3′. The primer set used for generating the Y656F mutant topo IIβ was 5′-CGC ATC TTG TTT AGA TTT GCT GGT CCT GAA GAT GAT GC-3′ and 5′-GC ATC ATC TTC AGG ACC AGC AAA TCT AAA CAA GAT GCG-3′. These cDNAs were cloned in the pHT212 plasmid and transformed in the *Saccharomyces cerevisiae* yeast strain, BJ201, for preparing recombinant protein for *in vitro* decatenation assay as described earlier (22,23). The cDNAs were also cloned in the neo-containing IRES-enhanced green fluorescent protein expression pEIE vector described earlier (8) for expressing the recombinant proteins in the genetically engineered fibrosarcoma cell line, HTETOP (25) and in the *m*-AMSA-resistant HL-60 cell line (HL-60/AMSA-R), which does not express the topo IIβ protein (8,26).

Cell lines stably expressing WT or mutant topo II isoform or topo II isoform-targeted shRNA

The HTETOP cell line described earlier (25) is a genetically engineered HT1080 cell line in which both alleles of topo IIα are disrupted and the cells are stably transfected with an exogenous topo IIα cDNA (referred to as parental topo IIα) controlled by the Tet transactivator (tTA). These cells were cultured in advanced DMEM (Life Technologies, Carlsbad, CA) supplemented with 2 mM L-glutamine (Life Technologies, Carlsbad, CA, USA) and 10% fetal bovine serum (Atlanta Biologicals Inc., Lawrenceville, GA, USA)

in a humidified atmosphere of 5% CO_2 and 95% air. Although these cells are not viable in the presence of Tet due to silencing of >99.5% topo IIα expression and low levels of endogenous topo IIβ expression, Tet-resistant clones can be selected after stable transfection with expression plasmids of either topo IIα or topo IIβ (27). Accordingly, HETEOP cells were transfected with the WT or mutant topo IIα or topo IIβ expression plasmids described above and the transfected cells were selected in the presence of 1 μg/ml Tet in advanced DMEM supplemented with 2 mM L-glutamine and 10% fetal bovine serum. Once selected the stably transfected cells were grown in the presence or absence of Tet to express either the transfected topo II isoform alone or the transfected topo II isoform plus the parental Tet-regulated topo IIα protein, respectively. Prior to initiation of any experiment, cells were cultured in the experimental condition (+ Tet or –Tet) for at least 2 weeks. Supplementary Table S1 and Supplementary Figure S1 show the expression of the specific topo II isoforms in the presence or absence of Tet for each cell line.

Construction of HL-60 cells (ATCC, Manassas, VA, USA) stably transfected with topo IIα or topo IIβ sh-RNA (HL-60/si-topo IIα or HL-60/si-topo IIβ, respectively) as well as the HL-60/AMSA-R stably transfected with WT topo IIβ cDNA (HL-60/AMSA-R/topo IIβ) was previously described (8). Cultures of these HL-60 cells were maintained in RPMI-1640 supplemented with 10% fetal bovine serum and 2 mM L-glutamine at 37°C in a humidified atmosphere of 5% CO_2 and 95% air. Compared to control HL-60/siGFP cells, the degree of stable down regulation of topo IIα and topo IIβ in the HL-60/si-topo IIα and HL-60/si-topo IIβ cell lines was 72 ± 7.2% and 96 ± 4.1%, respectively (Supplementary Figure S2), even when these cell lines were maintained in the absence of the selection marker, puromycin. Mouse embryonic fibroblasts (MEF) $MEF^{\beta+/+}$ and $MEF^{\beta-/-}$, immortalized with simian virus 40 (SV40) large T antigen transformation were a generous gift from Dr Gloria Li, Memorial Sloan Kettering Cancer Center, New York, NY (12,28). The $MEF^{\beta+/+}$ and $MEF^{\beta-/-}$ cells were cultured in RPMI-1640 supplemented with 10% fetal bovine serum and 2 mM L-glutamine at 37°C in a humidified atmosphere of 5% CO_2 and 95% air.

Preparation of cell lysates and western blot analysis

Total cell lysates were prepared in radioimmunoprecipitation assay (RIPA) buffer as described earlier (23). Equivalent aliquots of cell lysates (10–20 μg) were electrophoresed on a 3–8% Tris–acetate gel (Life Technologies, Carlsbad, CA, USA), transferred to PVDF membrane and subjected to Western blot analysis with specific antibodies. Topo IIα and topo IIβ antibodies were used at a dilution of 1:2000, myc-tag protein antibody was used at a dilution of 1:2000 and HRP-conjugated antibody to actin was used at a dilution of 1:40000. Anti-rabbit IgG antibody, peroxidase labeled or anti-mouse IgG antibody, peroxidase labeled (SeraCare Life Sciences, Milford, MA, USA) diluted 1:40000 was used as the secondary antibody.

Determination of pseudomitotic index

HTETOP cells expressing WT or mutant forms of topo IIα or topo IIβ were grown on coverslips in 6 well plates to 60–70% confluence. The cells were then incubated without or with ICRF-193 (2 μM) for 2.5 h followed by incubation with 50 ng/ml of colcemid for 0.5 h. Cells were subsequently incubated with 2 ml of a hypotonic solution of 60% sodium citrate (0.8%)/40% potassium chloride (0.075 M) for 20 min at 37°C and fixed at 4°C with ice cold methanol/glacial acetic acid (3:1) for an additional 20 min. The cover slips were then mounted onto slides using Vectashield containing DAPI as the mounting media. The number of interphase nuclei as well as normal (absence of ICRF-193) or abnormal mitotic chromosomes (presence of ICRF-193) were counted using a fluorescent microscope. Approximately 700–1200 nuclei were counted per sample. In the absence of ICRF-193 the number of mitotic cells did not vary significantly in the parent HTETOP cells and the topo IIα or topo IIβ transfected cells (Supplementary Table S2). For HL-60 cells, the cell suspension was incubated without or with ICRF-193 plus colcemid under the conditions described for HTETOP cells. Following treatment with hypotonic solution of 60% sodium citrate (0.8%)/40% potassium chloride (0.075 M) for 20 min at 37°C and fixation at 4°C with ice cold methanol/glacial acetic acid (3:1), an aliquot of the fixed cells was dropped onto a glass slide, air dried and mounted with Vectashield. Pseudomitotic index was calculated as the frequency of pseudomitosis in ICRF-193 plus colcemid treated cells divided by the frequency of mitosis in colcemid treated cells and expressed as a percentage (29). This procedure provides a better estimate of the decatenation checkpoint, compared to the one employing determination of mitotic cells by mitosis-associated phospho-histone H3 staining, since entangled chromosomes would be expected to be observed only for a defective decatenation checkpoint, but not a defective DNA damage checkpoint.

Determination of activation of the DNA damage checkpoint

The activation of the DNA damage checkpoint was determined by examining percent phosphorylation of H2AX using the Muse H2AX activation dual detection kit, essentially as described by the manufacturer. Following treatment of HTETOP transfected cells with DMSO for 3 h, 2 μM ICRF-193 for 3 h or 5 μM VP-16 for 1 h, 2.5 × 10^6 cells were fixed, permeabilized and incubated with a pair of phospho-specific anti-phospho-histone H2AX (Ser139)-Alexa Fluor 555 conjugated antibody and anti-Histone H2A.X PECy5 conjugated antibody (that detects total levels of Histone H2AX) in multiplex. Use of the two antibodies in multiplex allowed for normalization of the total and phospho levels to accurately estimate the level of H2AX activation. The stained cells were analyzed by the MUSE Cell Analyzer which estimated the percentage of activated (staining positive with the phospho-specific H2AX antibody) and inactivated cells (staining positive only with the anti-Histone H2AX antibody). This information was employed to calculate percent active cells relative to total number of H2AX expressing cells.

Cell sorting and flow cytometry

HTETOP cells ectopically expressing WT topo IIβ and maintained in 1 μg/ml Tet had sub-populations of diploid and aneuploid cells (Supplementary Figure S3). To isolate the diploid population, cells were stained with 4 μg/ml Hoechst 33342 for 30–45 min at 37°C, centrifuged and re-suspended at 2×10^6 cells/ml in advanced DMEM supplemented with 10% fetal bovine serum and 2 mM L-glutamine. Sorting of the diploid population was carried out in an ICyte Reflection (BD Biosciences, San Jose, CA). The gated region set for the diploid population based on the Hoechst 33342 fluorescence distribution histogram represented 10.1% of the 16.1% gate set. From the 3.9×10^6 detected events, 0.31×10^6 cells represented the total sorted diploid population. Sorted diploid cells were subsequently cultured in advanced DMEM supplemented with 10% fetal bovine serum and 2 mM L-glutamine in the absence or presence of 1 μg/ml Tet. Ploidy and cell cycle phase distribution analysis was carried out in a Beckman Coulter XL (Beckman Coulter, Indianapolis, IN) following staining with propidium iodide.

Decatenation of κDNA by purified topo II

In vitro enzymatic activity of recombinant WT or mutant topo IIα or topo IIβ protein expressed in *S. cerevisiae* yeast strain, BJ201, (22,23) was assayed by measuring the decatenation of κDNA in a reaction mixture containing 50 mM Tris-HCl, pH 7.9, 88 mM KCl, 10 mM $MgCl_2$, 0.5 mM EDTA, 10 mM ATP, 10 mM dithiothreitol, 100 μg/ml bovine serum albumin and 150 ng of *k*DNA. At the end of the desired incubation period the reaction was stopped with 5% SDS and an aliquot of the reaction mixture was subjected to agarose (1%) gel electrophoresis. The gel was stained with ethidium bromide and the amount of decatenated minicircles of *k*DNA was quantified using an AlphaInnotech Image Analyzer (AlphaInnotech Corp., San Leandro, CA). Specific activity of topo II purified by Ni^{2+}-nitrilotriacetic acid-agarose column chromatography (23) was calculated as percent decatenation/pmol of topo II/min. The relative amount of topo II in the purified preparations was determined as previously described (23).

Determination of anti-tumor drug sensitivity

HTETOP cells expressing WT or mutant topo IIα or topo IIβ, or HL-60/siGFP, HL-60/si-topo IIα, HL-60/si-topo IIβ, HL-60/AMSA-R or HL-60/AMSA-R/topo IIβ cells were incubated with varying concentrations of VP-16 or *m*-AMSA for 1 hour at 37°C. Following treatment, HTETOP cells were washed and incubated in drug-free medium for 96 hours and viable cell counts determined. For HL-60 cells, following drug treatment cells were washed and plated on soft-agar plates and colonies counted after 7 days (6).

Statistical analysis

Statistical analysis was performed on data sets and significant differences were determined by T-test or Two-way ANOVA followed by Student-Newman-Keuls *post-hoc* tests when significance was detected.

Crystal structure and CTD sequence analysis

Using the published crystal structure of topo IIα (30) all atom-to-atom distances within 4.5Å were measured between two regions [(**R-1 (**593-IVKA…GTST-636**)** that corresponds to a folded 'Greek key'-like motif in topo IIα; **R-2 (**696-LPEQ…YGTA-705**)** that corresponds to an unstructured loop in topo IIα] with the rest of the amino acids in the topo IIα dimer. These two regions are missing in the published crystal structures of topo IIβ (31,32), but not in the crystal structure of topo IIα. To do the same measurements for the topo IIβ dimer, the TOPRIM (topoisomerase-Primase) domains of both isoforms were superimposed in PyMol (RMS = 0.5Å) and then to the R-1 and R-2 regions, in topo IIβ, were assigned the coordinates of their counterparts from topo IIα, by homology modelling.

The consensus secondary structure prediction for topo IIα and topo IIβ as previously described (33) and sequence propensities for various PTMs for topo IIα and topo IIβ CTD were generated. In addition, sequence propensity for intrinsic disorder was scaled to a 0–9 score as described earlier (34). The similarity score was calculated based on the alignment of the two CTD sequences, using an in-house script with an implemented BLOSUM62 matrix.

RESULTS

Topo IIα and topo IIβ are required for the decatenation checkpoint

Fidelity of the decatenation checkpoint is essential for maintaining chromosomal integrity and limited information is available on the role of topo IIβ in regulating this critical checkpoint. To test the role of topo IIα and topo IIβ in regulating the decatenation checkpoint we used three different model systems that differentially express the two isoforms. These included the human HTETOP and HL-60 cell lines and the SV40 transformed MEF cell line described in 'Materials and Methods'. The decatenation checkpoint was assessed by measuring the pseudomitotic index, which corresponds to the ratio of the frequency of pseudomitosis (cells entering mitosis with entangled chromosomes) in cells treated with the topo II catalytic inhibitor, ICRF-193, to the frequency of mitosis in untreated cells (29). A higher value is indicative of a defective checkpoint, since cells enter mitosis in the presence of entangled chromosomes. As shown in Figure 1A, the pseudomitotic state with entangled chromosomes was observed in ICRF-193 treated topo IIα- or topo IIβ-transfected HTETOP cells in which expression of parental Tet-regulated topo IIα was suppressed by Tet. In these cells normal mitotic chromosomes were rarely observed and if present, the frequency was <0.1% (Supplementary Table S3). However, the pseudomitotic index in WT topo IIβ-transfected HTETOP cells (+Tet) expressing only WT topo IIβ was lower compared to that in WT topo IIα-transfected HTETOP cells (+Tet) or the parent HTETOP cell line (-Tet), predominantly expressing WT topo IIα and low levels of endogenous topo IIβ (Figure 1B). No significant difference in the pseudomitotic index was observed between WT topo IIα-transfected cells and the parent HTETOP cell line (Figure 1B). In addition to determining activation of the decatenation checkpoint following inhibition of

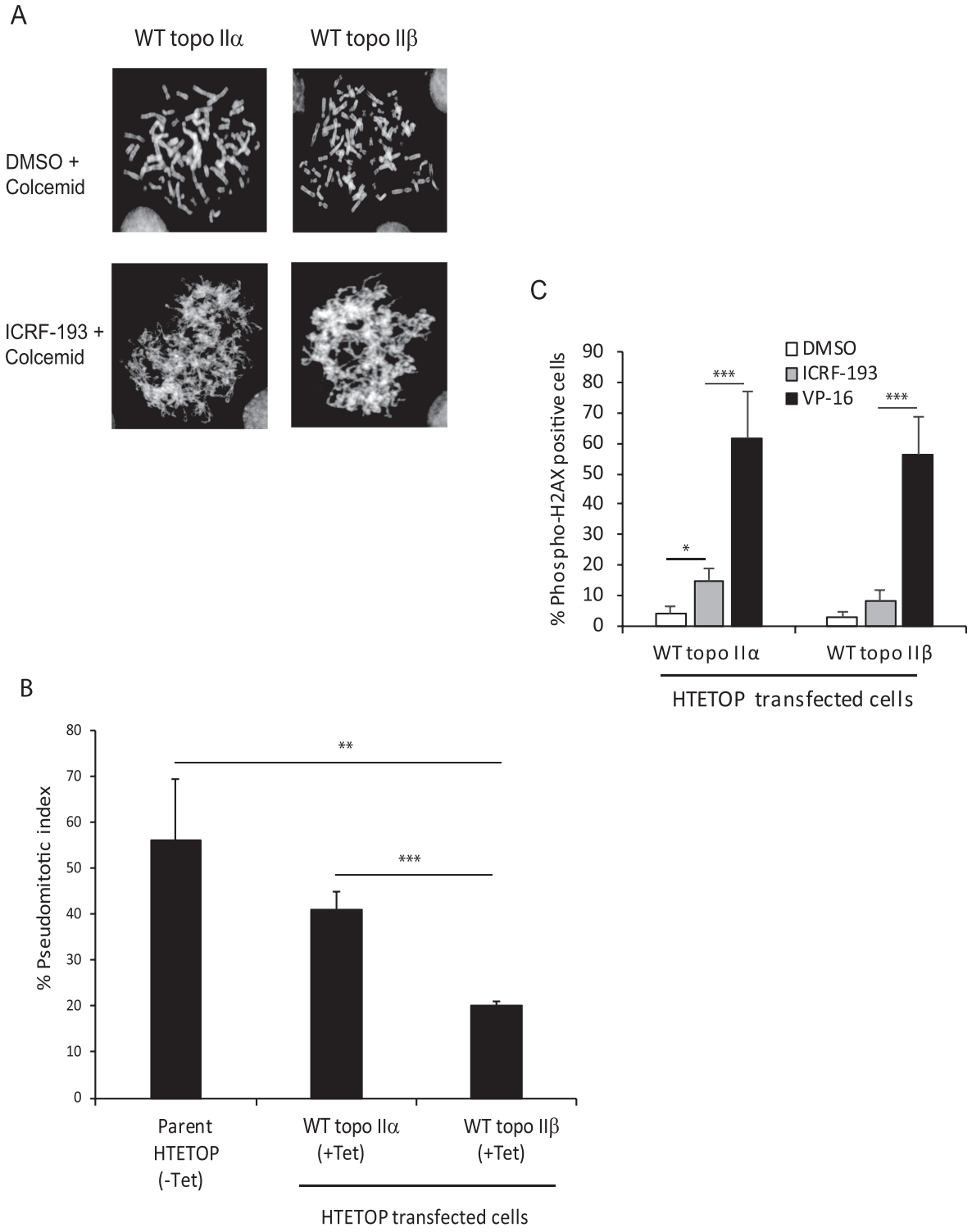

Figure 1. Topo IIβ is more proficient than topo IIα in regulating the decatenation checkpoint. (A) Representative metaphase spreads of normal mitotic chromosomes and pseudomitotic entangled chromosomes in WT topo IIα or WT topo IIβ-transfected HTETOP cells grown in the presence of 1μg/ml Tet and treated without or with 2 μM ICRF-193 for 2.5 h followed by 50 ng/ml colcemid for 0.5 h. (B) Quantification of the pseudomitotic index in the untransfected parent HTETOP cell line grown in the absence of Tet and in the WT topo IIα- and WT topo IIβ-transfected HTETOP cells grown in the presence of Tet. Columns represent the mean of three biological replicates and the bars indicate standard deviations. $^{**}P < 0.01$, $^{***}P < 0.001$ (two-sample t-test was used to compare data sets). (C) Determination of H2AX phosphorylation in WT topo IIα- and WT topo IIβ-transfected HTETOP cells treated with DMSO, ICRF-193 or VP-16. Columns represent the mean of at least three biological replicates and the bars indicate standard deviations. $^{*}P < 0.05$, $^{***}P < 0.001$ (two-sample t-test was used to compare data sets).

topo II catalytic activity by ICRF-193, we also determined whether this treatment led to activation of the DNA damage checkpoint by measuring phosphorylation of H2AX. Our results revealed that while the DNA-damaging agent VP-16 led to a significant increase in phospho-H2AX positive cells in both WT topo IIα- and WT topo IIβ-transfected HTETOP cells, ICRF-193 treatment led to no significant increase in topo IIβ-transfected HTETOP cells and a modest increase in topo IIα-transfected cells (Figure 1C). These results suggest that like topo IIα, the topo IIβ isoform, is also capable of regulating the decatenation checkpoint and may do so more proficiently than topo IIα.

The decatenation checkpoint is more efficient when both topo IIα and topo IIβ are present

The topo IIα-and topo IIβ-transfected HTETOP cells are aneuploid based on chromosome number and flow cytometry DNA profiles (Figures 1A, 2A and Supplementary Figure S3). Comparison of the DNA distribution profiles of the topo IIα and topo IIβ transfected HTETOP cells with that of the diploid HL-60 cell line revealed that while the majority of the cell population of the topo IIα transfected HTETOP cell line was aneuploid (Supplementary Figure S3), a small, but distinct, sub-population of the topo IIβ transfected HTETOP cell line was diploid (Figure 2A and Supplementary Figure S3). This population when purified by cell sorting resulted in cells that were primarily diploid (Figure 2A, B and Supplementary Figure S4). Following culture of the sorted diploid population as well as the unsorted aneuploid population in the absence or presence of Tet, cells expressing both topo IIα and topo IIβ or only topo IIβ, respectively were tested for their ability to regulate the decatenation checkpoint. The results (Figure 2C) revealed that the pseudomitotic index of cells expressing both topo IIα and topo IIβ (-Tet) was significantly lower ($P = 0.002$, two-way ANOVA) than that of cells expressing only topo IIβ (+Tet). For the sorted diploid cell population a 3-fold decrease ($P = 0.005$) in the pseudomitotic index was observed for cells expressing both topo IIα and topo IIβ (-Tet), compared to those expressing only topo IIβ (+Tet). For the unsorted aneuploid cell population a 1.6-fold decrease ($P = 0.055$) in the pseudomitotic index was observed for cells expressing both topo IIα and topo IIβ (-Tet), compared to those expressing only topo IIβ (+Tet). However, no significant difference was observed in the pseudomitotic index of topo IIα-transfected HTETOP cells cultured in the absence or presence of Tet (Figure 2D), despite higher level (approximately 2-fold) of expression of topo IIα in cells cultured in the absence of Tet. Our findings thus indicate that efficient regulation of the decatenation checkpoint requires both topo II isoforms.

Consistent with the observations in HTETOP cells, the decatenation checkpoint in other model systems revealed similar findings. Stable down regulation (8, Supplementary Figure S2) of either topo IIα (72 ± 7.2%) or topo IIβ (96 ± 4.1%) in HL-60 cells (HL-60/sitopo IIα or HL-60/sitopo IIβ, respectively) led to an increase in the pseudomitotic index compared to control cells (HL-60/siGFP) (Figure 3A), confirming that the decatenation checkpoint is regulated by both topo IIα and topo IIβ and is most efficient when both isoforms are present. Our results demonstrating a higher pseudomitotic index in topo IIβ-deficient cells (HL-60/si-topo IIβ), which express higher levels of topo IIα and lower levels of topo IIβ compared to topo IIα-deficient cells, supports our finding in HTETOP cells that the topo IIβ isoform may be more proficient in regulating the decatenation checkpoint. However, it is possible that differential down regulation of topo IIα (72%) and topo IIβ (96%) in the HL-60/si-topo IIα and HL-60/si-topo IIβ cell lines, respectively could have contributed to the lower pseudomitotic index observed in HL-60/si-topo IIα cells. A high pseudomitotic index was also observed in the amsacrine resistant HL-60 cell line (HL-60/AMSA-R), which does not express topo IIβ (Figure 3B). Nevertheless, re-expression of topo IIβ in the HL-60/AMSA-R cell line (HL-60/AMSA-R/topo IIβ) led to a 4-fold decrease in the pseudomitotic index (Figure 3B), confirming the role of topo IIβ in the decatenation checkpoint. The pseudomitotic index in topo IIβ$^{-/-}$ mouse embryo fibroblasts (MEF) was also found to be significantly higher than in topo IIβ$^{+/+}$ fibroblasts (Figure 3C). The relatively high pseudomitotic index observed in the topo IIβ$^{+/+}$ MEF cells, which express both topo IIα and topo IIβ, could be due to transformation of these cells by the SV40 large T antigen, which is known to destabilize the genome.

Deletion of the CTD, while preserving the nuclear localization signal (NLS), differentially modulates the in vitro decatenation activity and decatenation checkpoint whereas mutation of homologous tyrosines, Y640 in topo IIα and Y656 in topo IIβ, attenuates these activities

Since the CTDs of topo IIα and topo IIβ share little homology and are not directly involved in the catalytic activity, it has been suggested that they are involved in regulating the divergent cellular functions of these isoforms. Therefore, we tested C-terminal deletion mutants of topo IIα and topo IIβ on the in vitro catalytic activity and decatenation checkpoint. For determining this we deleted most of the CTD but retained the region corresponding to the NLS, since the topo II isoforms function in the nucleus. Whereas, deletion of the CTD of topo IIα led to an approximate 8-fold increase in the decatenation activity compared to WT topo IIα (Table 1 and Supplementary Figure S5), deletion of the CTD of topo IIβ resulted in an approximate 10-fold decrease in the decatenation activity compared to WT topo IIβ (Table 1 and Supplementary Figure S6). Similarly, the pseudomitotic index of HTETOP cells transfected with C-del topo IIα was 5-fold lower than that of HTETOP cells transfected with WT topo IIα, even when the WT-topo IIα transfected cells cultured in the absence of Tet expressed higher levels of topo IIα (Figure 4A and Table 2). In contrast the pseudomitotic index of HTETOP cells expressing C-del topo IIβ was 1.5-fold higher than HTETOP cells expressing WT topo IIβ (Figure 4B).

Previously we reported that mutation of a non-catalytic tyrosine residue, Y656, in topo IIβ decreased its catalytic activity (22, Table 1 and Supplementary Figure S6). In this study we show that mutation of a homologous tyrosine, Y640, in topo IIα also decreased the in vitro decatenation activity of this isoform (Table 1 and Supplementary Figure S5). Consistent with this observation the pseudomitotic in-

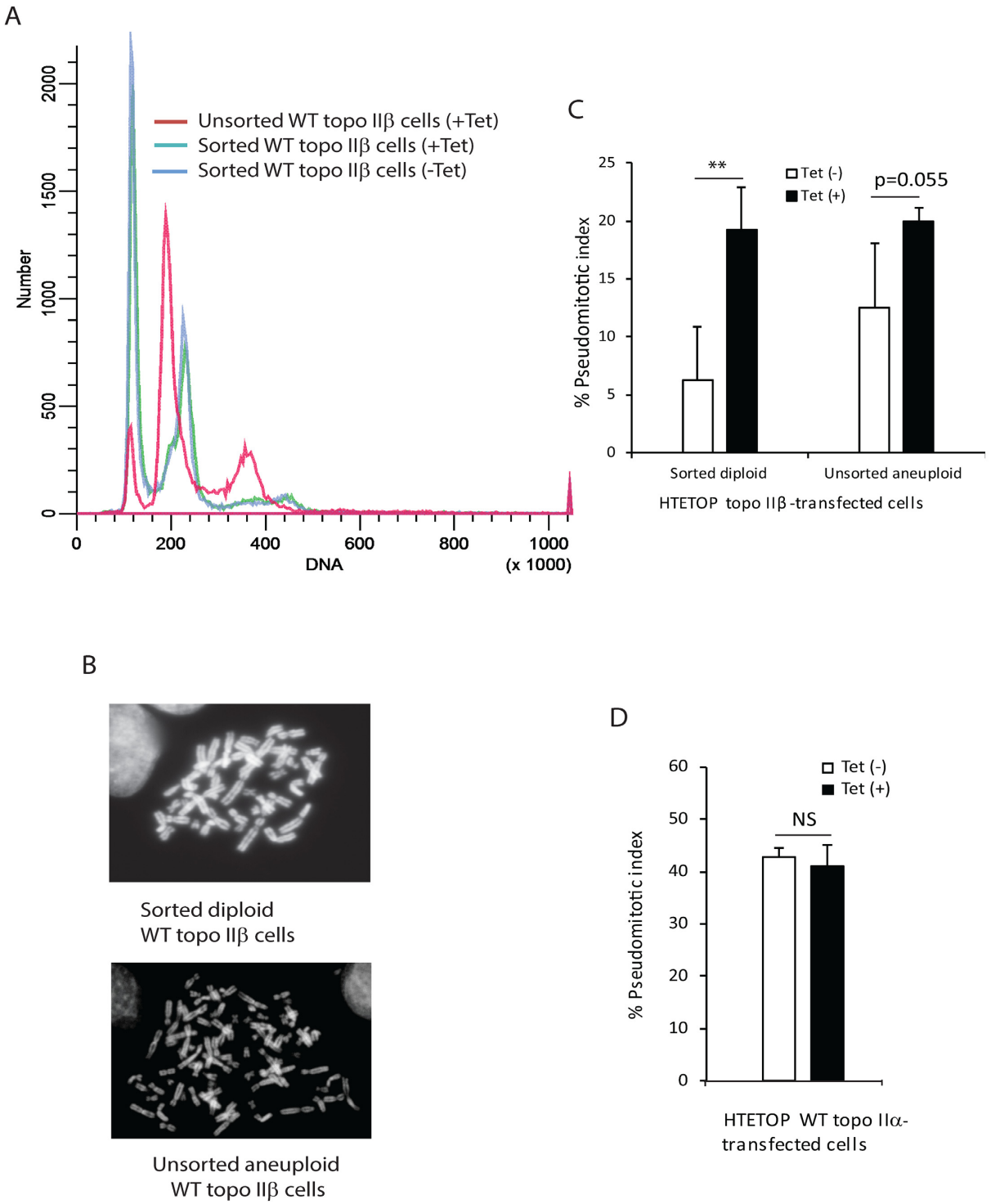

Figure 2. Efficient regulation of decatenation checkpoint requires expression of both topo IIα and topo IIβ. (A) Flow cytometry analysis of WT topo IIβ-transfected HTETOP cells prior to and following enrichment of the diploid population by cell sorting. The DNA distribution profile of the sorted population was identical when incubated in the absence or presence of Tet as seen by the superimposed blue and green lines. (B) Representative metaphase spreads of sorted diploid and unsorted aneuploid WT topo IIβ-transfected HTETOP cells. (C) Quantification of the pseudomitotic index of anueploid unsorted and sorted diploid WT topo IIβ-transfected HTETOP cells incubated in the absence or presence of 1 μg/ml Tet. Columns represent the mean of three biological replicates and the bars indicate standard deviations. $^{**}P < 0.01$ (two-way ANOVA, Student-Neuman-Keuls post-hoc test). (D) Quantification of the pseudomitotic index of unsorted aneuploid topo IIα-transfected HTETOP cells incubated in the absence or presence of 1 μg/ml Tet. Columns represent the mean of three biological replicates and the bars indicate standard deviations. NS, not significant (two-sample t-test was used to compare data sets).

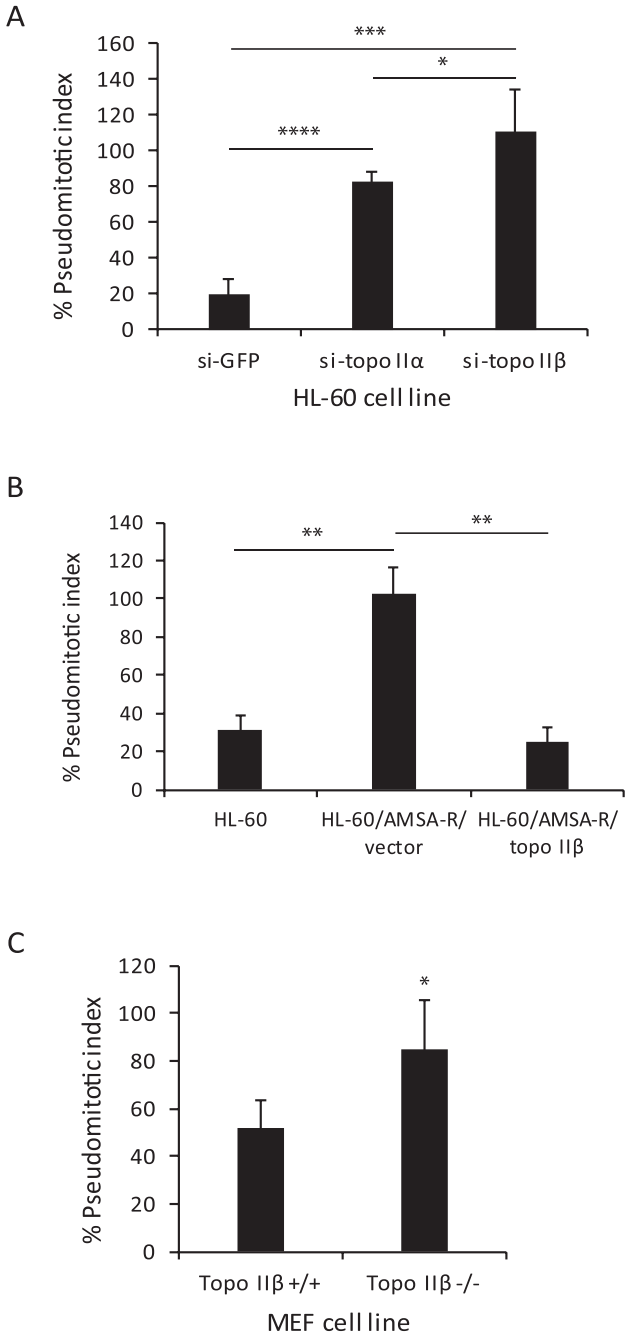

Figure 3. Deficiency of topo IIα and topo IIβ impairs the decatenation checkpoint in HL-60 and MEF cells. (A) Pseudomitotic index of HL-60 cells stably transfected with shRNAs targeted to GFP (HL60/si-GFP), topo IIα (HL60/si-topo IIα) or topo IIβ (HL60/si-topo IIβ). Columns represent the mean of three biological replicates and the bars indicate standard deviations. $*P < 0.05$, $***P < 0.001$, $****P < 0.0001$ (two-sample t-test was used to compare data sets). (B) Pseudomitotic index of parental HL-60, HL-60/AMSA-R/vector or HL-60/AMSA-R/topo IIβ cells. Columns represent the mean of three biological replicates and the bars indicate standard deviations. $**P < 0.01$ (two-sample t-test was used to compare data sets). (C) Pseudomitotic index of MEF topo IIβ +/+ and topo IIβ -/- cells. Columns represent the mean of three biological replicates and the bars indicate standard deviations. $*P < 0.05$ (two-sample t-test was used to compare data sets).

Table 1. Specific activities of WT and mutant topo II isoforms

Topo II protein	Specific activity (relative % decatenation/pmol/min)	
	Topo IIα	Topo IIβ
WT	32.3 ± 14	34.9 ± 8
C-del mutant	273.4 ± 45.3	3.6 ± 2.1
Tyrosine mutant	7.9 ± 2	3.8 ± 1.5

Table 2. Pseudomitotic index of topo II-transfected HTETOP cells in the presence or absence of Tet

Topo II-transfected HTETOP cell line	Pseudomitotic index	
	Tet (+)	Tet (-)
WT topo IIα	41.03 ± 3.98	42.77 ± 1.57
C-del topo IIα	8.32 ± 5.96	7.78 ± 3.93
Y640F topo IIα	86.15 ± 22.99	44.61 ± 4.27
WT topo IIβ	20.01 ± 1.11	12.50 ± 5.6
C-del topo IIβ	30.66 ± 2.17	29.85 ± 1.78
Y656F topo IIβ	66.33 ± 16.47	39.37 ± 10.54

dex of HTETOP cells expressing Y640F mutant topo IIα or Y656F mutant topo IIβ was significantly higher than cells expressing WT topo IIα or WT topo IIβ, respectively (Figure 4A and B). Specifically, a 2.1-fold increase and 3.4-fold increase compared to the WT enzyme was observed for the Y640F topo IIα and Y656F topo IIβ mutation, respectively. Interestingly, the pseudomitotic index of Y640F mutant topo IIα- and Y656F mutant topo IIβ-transfected HTETOP cell lines in the absence of Tet was lower when compared to that in the presence of Tet and was similar to that observed for the parental or WT topo IIα transfected cells (Table 2). However, the pseudomitotic index of C-del topo IIα- or C-del topo IIβ-transfected cells in the presence of Tet, which was lower than that of WT topo IIα-transfected cells, was unaffected when these cells were cultured in the absence of Tet (Table 2). These findings suggest that although the CTDs of topo IIα and topo IIβ reciprocally modulate the in vitro and in vivo decatenation activity of these isoforms, the homologous non catalytic tyrosine residues (Y640 in topo IIα and Y656 in topo IIβ) similarly influences the in vitro and in vivo decatenation activities of these isoforms.

To determine whether ICRF-193 led to DNA damage we examined phosphorylation of H2AX following treatment with ICRF-193 in the WT and mutant topo IIα- and topo IIβ-transfected cells. These studies revealed that while ICRF-193 led to a modest phosphorylation of H2AX (approximately 7%) in all transfected cell lines (Figure 4C and D), no statistically significant differences were observed in H2AX phosphorylation between the different cell lines (two-way ANOVA, Student-Neuman-Keuls post-hoc test). In contrast the DNA damaging agent, VP-16 led to significantly higher phosphorylation of H2AX in all transfected cell lines ($P < 0.001$, two-way ANOVA, Student-Neuman-Keuls post-hoc test) (Figure 4C and D). However, no statistically significant differences (two-way ANOVA, Student-Neuman-Keuls post-hoc test) were observed in H2AX phosphorylation between the different cell lines treated with VP-16.

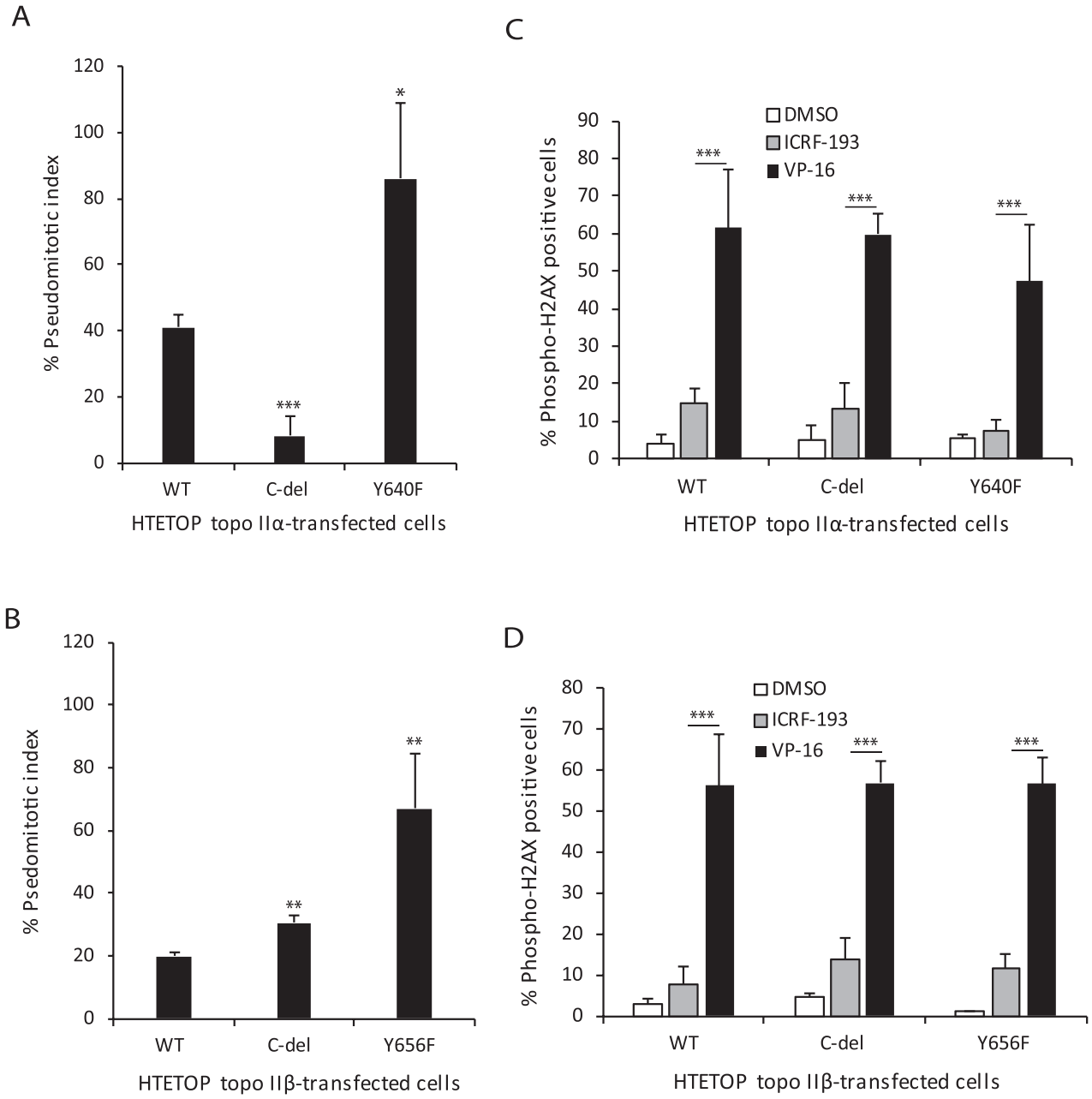

Figure 4. Deletion of the CTD of topo IIα or topo IIβ or mutation of the homologous tyrosine Y640F in topo IIα or Y656F in topo IIβ dysregulates the decatenation checkpoint. (A) Pseudomitotic index of HTETOP cells expressing WT, C-del or Y640F mutant topo IIα. Columns represent the mean of three biological replicates and the bars indicate standard deviations. $*P < 0.05$, $**P < 0.001$ (two-sample t-test was used to compare WT topo IIα-transfected cells to C-del topo IIα-transfected cells or Y640F mutant topo IIα-transfected cells). (B) Pseudomitotic index of HTETOP cells expressing WT, C-del or Y656F mutant topo IIβ. Columns represent the mean of three biological replicates and the bars indicate standard deviations. $**P < 0.01$ (two-sample t-test was used to compare WT topo IIβ-transfected cells to C-del topo IIβ-transfected cells or Y640F mutant topo IIβ-transfected cells). (C) Determination of H2AX phosphorylation in HTETOP cells expressing WT, C-del or Y640F mutant topo IIα that were treated with DMSO, ICRF-193 or VP-16. Columns represent the mean of at least three biological replicates and the bars indicate standard deviations. $***P < 0.001$ (two-way ANOVA, Student-Neuman-Keuls post-hoc test). (D) Determination of H2AX phosphorylation in HTETOP cells expressing WT, C-del or Y656F mutant topo IIβ that were treated with DMSO, ICRF-193 or VP-16. Columns represent the mean of at least three biological replicates and the bars indicate standard deviations. $***P < 0.001$ (two-way ANOVA, Student-Neuman-Keuls post-hoc test).

Deletion of the CTD of topo IIα or topo IIβ or mutation of Y640 in topo IIα or Y656 in topo IIβ alters anti-tumor drug sensitivity

Since topo II is an effective clinical target for several chemotherapeutic drugs we wanted to determine the effect of deletion of the CTD or mutation of the homologous non-catalytic tyrosine on drug sensitivity. Therefore, we first tested selectivity of two clinically useful anti-tumor drugs, VP-16 and *m*-AMSA, for topo IIα or topo IIβ in HL-60 cells differentially expressing these isoforms. Our results revealed that HL-60/si-topo IIα cells that are deficient in topo IIα are significantly more resistant to the cytotoxic effects of VP-16, compared to control HL-60/siGFP cells and HL-60/si-topoIIβ cells that are deficient in topo IIβ (Figure 5A). In contrast, HL-60/si-topo IIβ cells that are deficient in topo IIβ are significantly more resistant to *m*-AMSA compared to the HL-60/siGFP and HL-60/si-topoIIα cells (Figure 5B). Similarly the HL-60/AMSA-R cells are more resistant to *m*-AMSA compared to the parent HL-60 cell line (Figure 5C). However ectopic expression of topo IIβ in the HL-60/AMSA-R cells sensitizes these cells to *m*-AMSA (Figure 5C). These data demonstrate that VP-16 and *m*-AMSA preferentially target topo IIα and topo IIβ, respectively.

Based on the selectivity of the topo II-targeted drugs, VP-16 and *m*-AMSA for topo IIα and topo IIβ, respectively we examined the sensitivity of HTETOP cells expressing WT or mutant forms of topo IIα or topo IIβ to these drugs. Whereas VP-16 cytotoxicity is significantly enhanced in cells expressing C-del topo IIα, VP-16 cytotoxicity is significantly diminished ($P < 0.006$ at VP-16 >2.5 μM) in cells expressing the Y640F mutant enzyme (Figure 6A). In contrast cells expressing C-del topo IIβ as well as cells expressing Y656F mutant topo IIβ are significantly more resistant to the cytotoxic effects of *m*-AMSA compared to cells expressing the WT enzyme (Figure 6B). Thus the decatenation checkpoint (Figure 4), in vitro catalytic activity (Table 1 and Supplementary Figures S5 and S6) and the cytotoxic effects of topo II-targeted drugs (Figure 6) are similarly regulated by the C-terminal region and the homologous non-catalytic tyrosine of topo IIα and topo IIβ.

Structural analysis of topo IIα and topo IIβ

Since the CTD of topo IIα and topo IIβ is intrinsically disordered and the crystal structure for this region is not available we performed structural alignment of this region to determine whether differences in structural features of topo IIα and topo IIβ could provide insights into the observed differential effect of the CTDs on topo II activity. As seen in Figure 7A the CTD of topo IIβ is longer with the extra 77 amino acids located in eight major insertions separating predicted secondary structure elements. Starting from amino acid approximately 1385, the last four insertions toward the C-terminus are highly negatively charged and contain multiple phenylalanines. Since acidic amino acids have the lowest DNA interaction propensity (35) and phenylalanine is known to interact more avidly with proteins than DNA this observation suggests the CTD of topo IIβ is prone to protein-protein rather than protein-DNA interactions, at least in the final C-terminal region. Further, prediction of PTMs and recent mass spectrometry based experimental results (36–38) indicate that the CTD is heavily modified post-translationally by SUMOylation, ubiquitination and phosphorylation, suggesting that this domain is involved in multiple protein-protein interactions. Interestingly, in the case of topo IIβ many of the modified amino acids are found in the insertions: 2 ubiquitination (K1294, K1297) and 5 phosphorylation (T1287, S1395, T1398, T1570, S1571) sites; or right next to the insertions: 1 SUMOylation (K1266), 2 ubiquitination (K1209, K1569) and 4 phosphorylation (S1419, S1436, S1447, S1576) sites. This suggests that topo IIβ CTD might recruit/interact with more proteins to enhance the decatenation activity, which in part might explain the attenuation of topo IIβ activity when the CTD is deleted.

Structural modeling analysis and evaluation of the available crystal structure of the topo IIα isoform (30), which preferentially decatenates positive supercoiled DNA (39) in 60° crossover geometry (40), revealed that the alignment of topo IIα CTD restricts passage of the transport (T) DNA through the G gate (Figure 7B and Supplementary Figure S7). Thus removal of the CTD of topo IIα would allow the T-segment to pass through the G-gate by simple diffusion, potentially explaining increased topo IIα activity following C-terminal deletion.

Since both Y640 in topo IIα and Y656 in topo IIβ are required for the efficient activation of the decatenation checkpoint, we performed structural analysis of the TOPRIM domain surrounding this region. As seen in Figure 7B the DNA crossover geometries in topo IIα and topo IIβ vary. In the negative supercoiled configuration of the DNA, which is preferred by topo IIβ, the T DNA will be on the direction and proximity of Y656 in the TOPRIM domain of topo IIβ. In contrast in the positive supercoiled configuration, which is preferred by topo IIα, the T DNA will be in proximity of the CTD. Further, comparison of the recent crystal structures of topo IIα (pdb: 4FM9) and topo IIβ (pdb: 3QX3, 4G0U, 4G0V, 4G0W, 4J3N) revealed two regions within the TOPRIM domain of topo IIβ that were missing in the electron density of all five topo IIβ structures (31,32). These missing regions are: **R-1**) 593-IVKA…GTST-636 - corresponding to a folded 'Greek key'-like motif in topo IIα and **R-2**) 696-LPEQ…YGTA-705 corresponding to an unstructured loop in topo IIα, close in space to Y640 in topo IIα (Supplementary Table S4 and Supplementary Figure S8). The absence of these regions in the electron density of topo IIβ indicates that they can be found in this isoform in multiple configurations. This may be due to some missing critical anchoring contacts with the rest of the protein, anchors that in turn are present in topo IIα, and/or to some configurational shifts induced by a stronger interaction with the T-segment DNA (Supplementary Table S4). One indication of missing anchoring contacts is that in the crystal structure of topo IIα the two regions (R-1 & R-2) are stabilized by a hydrogen bond between topo IIα E597-Y684. This contact is lost in topo IIβ, since Y684 is replaced by F700. Another possible anchor in topo IIα is the H-bond between S621 at the end of R-1 on one monomer with D963 in the DNA binding domain on the other monomer of the dimer, which is lost in topo IIβ as this serine is replaced with an alanine A637. The loss of favorable contacts is also shown by ho-

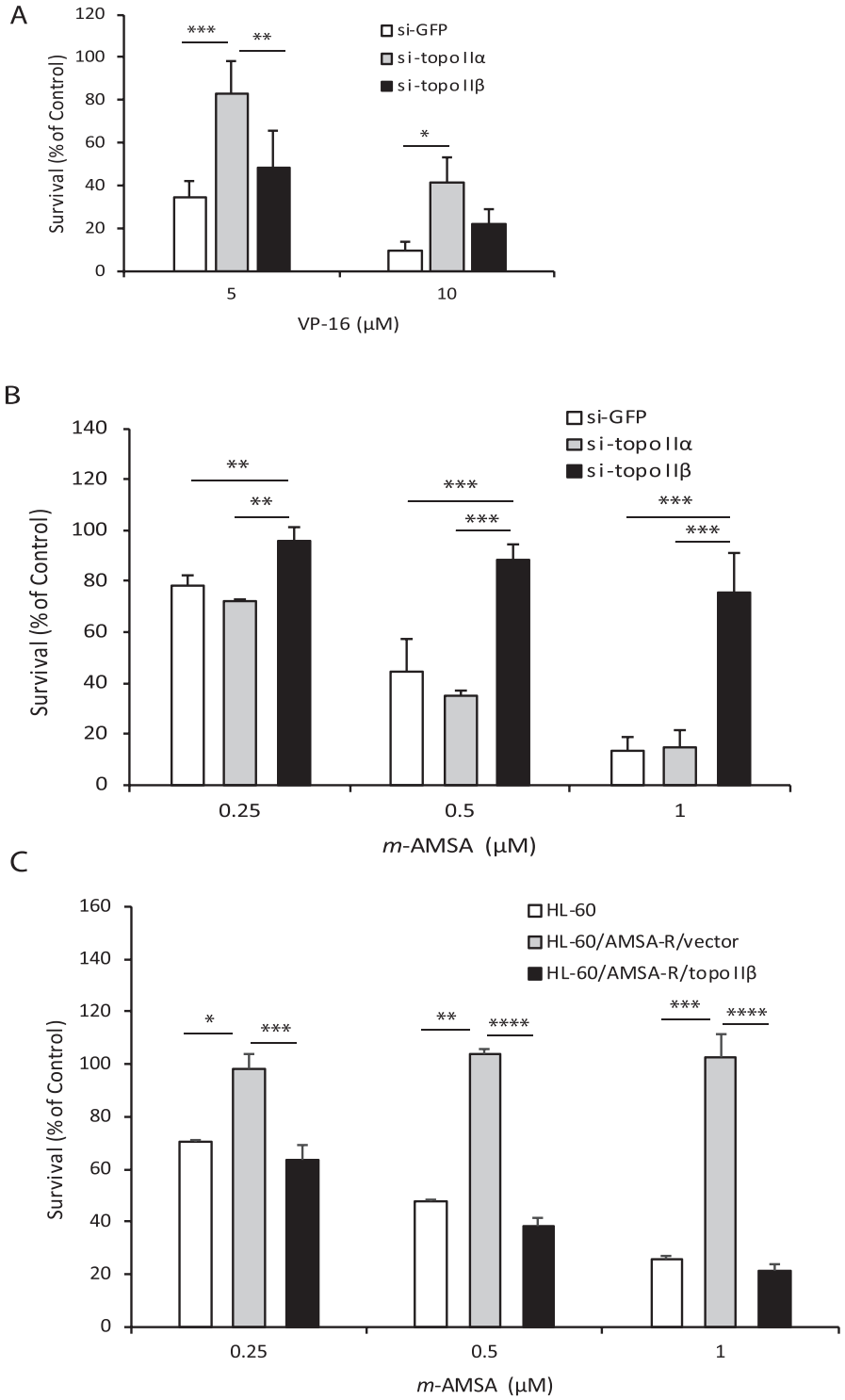

Figure 5. Topo II-targeted drugs VP-16 and m-AMSA preferentially target topo IIα and topo IIβ, respectively. (A) Survival of HL-60 cells transfected with shRNAs to GFP (HL60/si-GFP), topo IIα (HL60/si-topo IIα) or topo IIβ (HL60/si-topo IIβ) following treatment with varying doses of VP-16 for 1 h and growth in drug-free medium on soft-agar plates for 7 days. Columns represent the mean of three biological replicates and the bars indicate standard deviations. $^{*}P < 0.05$, $^{**}P < 0.01$, $^{***}P < 0.001$ (two-way ANOVA, Student-Neuman-Keuls post-hoc test). (B) Survival of HL-60 cells transfected with shRNAs to GFP (HL60/si-GFP), topo IIα (HL60/si-topo IIα) or topo IIβ (HL60/si-topo IIβ) following treatment with varying doses of *m*-AMSA for 1 hour and growth in drug-free medium on soft-agar plates for 7 days. Columns represent the mean of three biological replicates and the bars indicate standard deviations. $^{**}P < 0.01$, $^{***}P < 0.001$ (two-way ANOVA, Student-Neuman-Keuls post-hoc test). (C) Survival of parental HL-60, HL-60/AMSA-R/vector or HL-60/AMSA-R/topo IIβ cells following treatment with varying doses of *m*-AMSA for 1 hour and growth in drug-free medium on soft-agar plates for 7 days. Columns represent the mean of three biological replicates and the bars indicate standard deviations. $^{**}P < 0.01$, $^{***}P < 0.001$, $^{****}P < 0.0001$ (two-sample t-test was used to compare data sets).

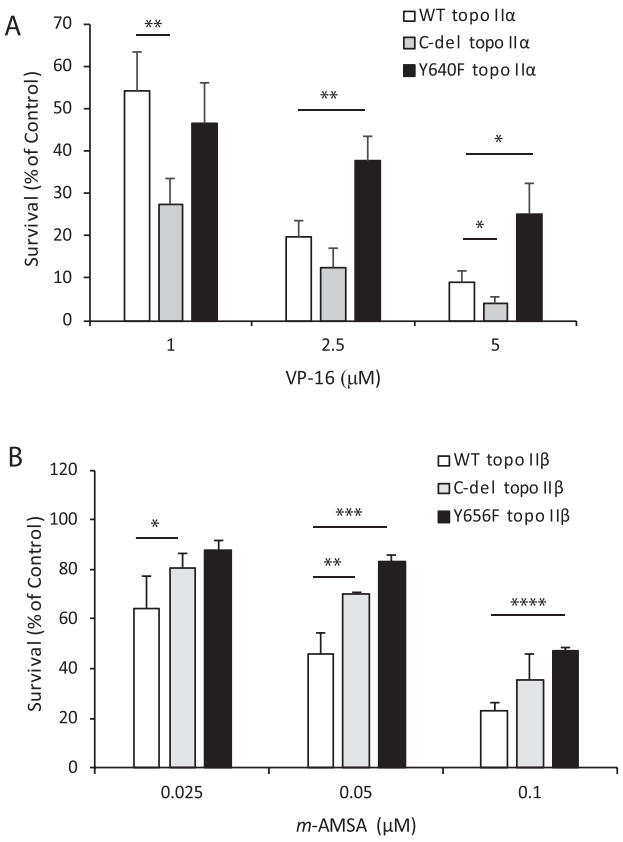

Figure 6. Deletion of the CTD of topo IIα or topo IIβ or mutation of the homologous tyrosine Y640F in topo IIα or Y656F in topo IIβ affects drug sensitivity. (A) Survival of HTETOP cells transfected with WT, C-del or Y640F mutant topo IIα following treatment with varying doses of VP-16 for 1 hour and incubation in drug-free medium for 96 hours. Columns represent the mean of three biological replicates and the bars indicate standard deviations. $*P < 0.05$, $**P < 0.01$ (two-sample t-test was used to compare data sets). (B) Survival of HTETOP cells transfected with WT, C-del or Y656F mutant topo IIβ following treatment with varying doses of *m*-AMSA for 1 hour and incubation in drug-free medium for 96 hours. Columns represent the mean of three biological replicates and the bars indicate standard deviations. $*P < 0.05$, $**P < 0.01$, $***P < 0.001$, $****P < 0.0001$ (two-sample t-test was used to compare data sets).

mology modeling. Assigning to the R-1 and R-2 regions in topo IIβ the coordinates of their counterparts in topo IIα by homology modeling, results in a significant loss of favorable contacts between R-1 and R-2 and the rest of the protein (Supplementary Table S4). Hence, in topo IIα there are more interactions contributing to the overall stability of these two regions. Interestingly also, surrounding these 'flexible' R-1 and R-2 regions, the number of basic amino acids in TOPRIM is increased in topo IIβ in comparison to topo IIα, (Supplementary Figure S8). Including the R-1 and R-2 segments in topo IIβ TOPRIM there are five additional positive charges with respect to topo IIα, while D683 of topo IIα is replaced by Q699 in topo IIβ. All these add up to an increased DNA interaction propensity of topo IIβ TOPRIM in comparison to topo IIα. A possible interpretation of this finding is that the T DNA might interact better and be aligned to TOPRIM in topo IIβ, in contrast to what happens in topo IIα.

DISCUSSION

In this study we demonstrate that topo IIα and topo IIβ isoforms, considered to be functionally distinct, can exhibit redundant activities. The topo IIβ isoform, in the absence of topo IIα, can support cell proliferation (this study, 27,41) and regulate the decatenation checkpoint. Our findings also indicate that activation of the decatenation checkpoint is more efficient when both topo IIα and topo IIβ are present. Although the CTD of topo IIα and topo IIβ as well as the homologous non-catalytic tyrosine residue (Y640 in topo IIα and Y656 in topo IIβ) play a role in regulating the decatenation checkpoint and drug sensitivity, deletion of most of the CTD, while preserving the NLS, reciprocally impacts topo IIα and topo IIβ function.

Previous reports have implicated a role for topo IIα in decatenation checkpoint (18–20), however most of these studies have not convincingly addressed the role of topo IIβ. In several of these studies activation of the checkpoint following treatment with the topo II catalytic inhibitor, ICRF-193, has been attributed to a role of topo IIα in decatenation checkpoint, despite the ability of ICRF-193 to inhibit both isoforms. However in this study we demonstrate that: (a) the decatenation checkpoint is preferentially regulated in HTETOP cells expressing only topo IIβ, compared to those expressing primarily topo IIα (Figure 1B), and (b) topo IIβ-deficient HL-60 cells expressing primarily topo IIα (Figure 3A) have a totally inefficient decatenation checkpoint. These findings provide evidence for a role of topo IIβ in the decatenation checkpoint and suggest that topo IIα alone may not efficiently activate this checkpoint. The ability of topo IIβ to regulate the decatenation checkpoint despite its degradation by ICRF-193 (40-50% after 1 h and 62–68% after 3 h, Supplementary Figure S9), suggests that prior to degradation, the topo IIβ circular clamp structure may be recognized by sensor proteins that initiate activation of the decatenation checkpoint signaling pathway. Alternatively, enough topo IIβ protein may be present following degradation by ICRF-193 to activate the decatenation checkpoint. The preferential role for topo IIβ in regulating the decatenation checkpoint is also consistent with studies demonstrating an inefficient decatenation checkpoint in stem and progenitor cells (29), which express relatively lower levels of topo IIβ as compared to topo IIα (42). In contrast differentiated cells, which have a more proficient decatenation checkpoint, express higher levels of topo IIβ compared to topo IIα (42). High expression of topo IIβ in granulosa cells of follicles has also been reported to be essential for regulating genomic integrity and follicle atresia (43). However, a previous study (19) in hTERT transformed normal human diploid fibroblasts expressing a decatenation defective topo IIβ showed that unlike topo IIα, topo IIβ is inefficient in regulating the decatenation checkpoint. This conclusion was based on their observation that siRNA-targeted depletion of topo IIα, but not topo IIβ, attenuated the decatenation checkpoint. Although the reason for this discrepancy is unclear at the present time, it is possible that the decatenation-defective topo IIβ present in their cells is unable to form the closed clamp topo II-DNA structural feature that would be recognized by checkpoint sensor proteins for activating the decatenation checkpoint in topo

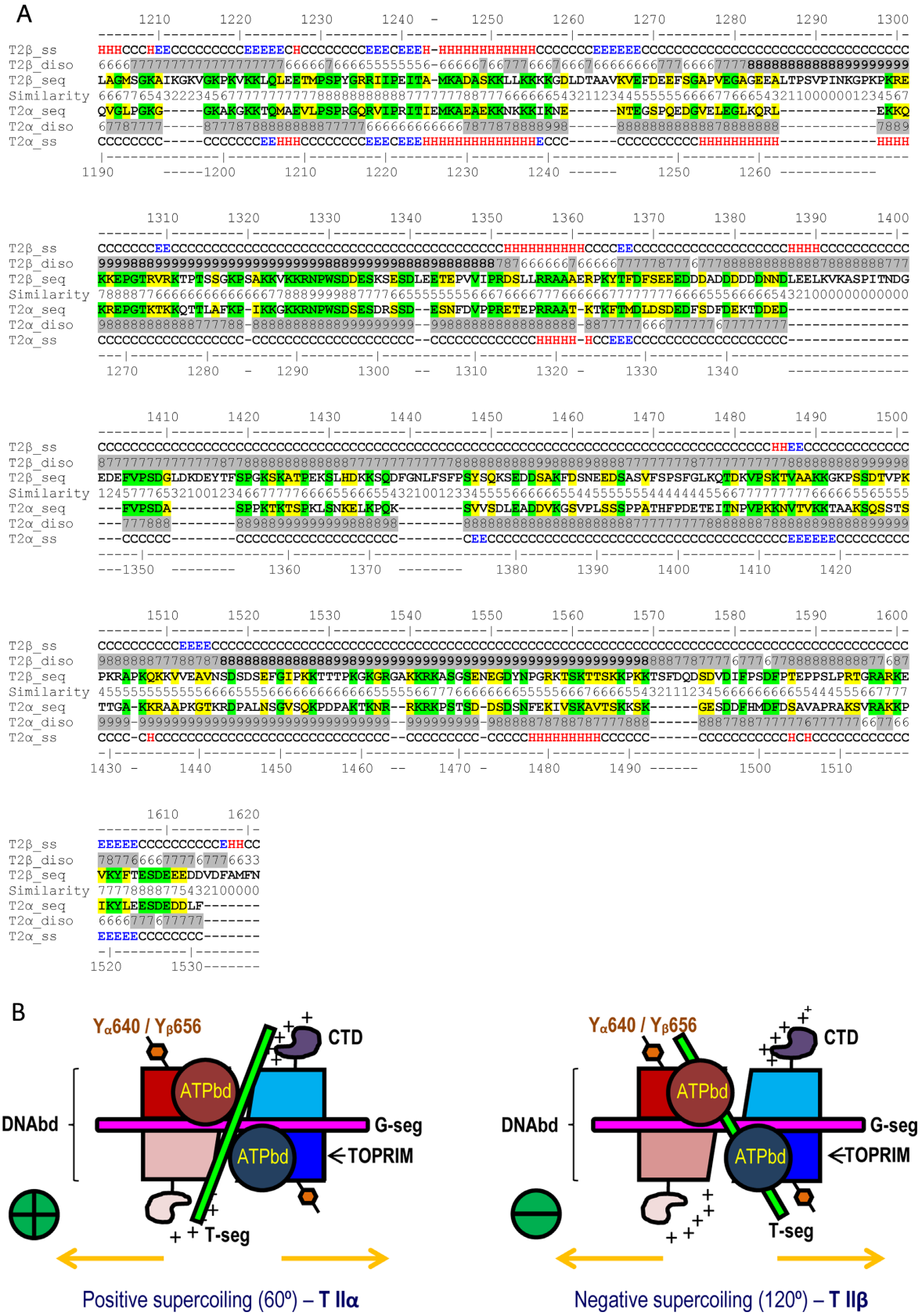

Figure 7. Structural comparison of topo IIα and topo IIβ proteins. (A) Sequence comparison of the CTD of topo IIα and topo IIβ. (B) Schematic model of the DNA crossover geometries in topoisomerase II illustrating the alignment of Y640 (topo IIα)/Y656 (topo IIβ) with respect to T DNA for positive and negative supercoiled DNA. The two monomers are represented in red and blue shades respectively.

IIα-deficient cells (17). Further, topo IIβ expression could also be compromised following degradation by ICRF-193 (44,45) during the 4–6 hr treatment interval used for measuring the mitotic entry rate.

It is not surprising for topo IIα and topo IIβ to exhibit overlapping functions given the essential nature of the topo II catalytic activity in DNA metabolic processes and cell survival. Thus, the functional activities of the two topo II isoforms could be dynamic and regulated uniquely within cells by distinct mechanisms, including PTMs e.g. phosphorylation and sumoylation, and protein interactions with nuclear protein complexes (21). These mechanisms could involve specific regions within the topo II protein, potentially the CTD given the divergence (22% identity) within this region between topo IIα and topo IIβ. Indeed our results of C-del topo IIα and topo IIβ, truncated at amino acids 1201 and 1219, respectively, and engineered to retain the NLS sequences (amino acids 1454–1497 for topo IIα and 1522–1573 for topo IIβ) demonstrated that the CTD of topo IIα and topo IIβ reciprocally regulated the in vitro (decatenation activity) and in vivo (decatenation checkpoint and sensitivity to topo II-targeted drugs) activities of these two isoforms. The C-del topo IIα isoform was significantly more efficient than full length topo IIα, whereas the C-del topo IIβ isoform was significantly less efficient than full length topo IIβ.

The present study directly evaluated the in vivo function of the C-terminal deleted mutants of topo IIα and topo IIβ, whereas other studies have examined the in vitro enzymatic activities of topo IIα truncated at different amino acids in the C-terminus region. Truncation of topo IIα at amino acid 1171 was shown to decrease the decatenation activity but enhance the DNA cleavage activity (46), which was comparable to the results observed for the topo II enzyme from Chlorella virus (47). In contrast, truncation of topo IIα at amino acid 1242 did not affect the decatenation activity (48). These differences may likely be due to deletions of the CTD at different amino acids. It is also possible that our results demonstrating differential regulation of topo IIα and topo IIβ functional activity by the CTD are due to the presence of the NLS. However, the CTD is less divergent in the NLS (approximate homology 42%) compared to the rest of this region, which suggests that regions other than the NLS may be more important in regulating enzyme function.

Whereas our study examined the in vivo functional role of the CTD of topo IIα and topo IIβ by expressing a C-terminal deleted enzyme that can be translocated to the nucleus, Linka et al (27) studied the in vivo role of the C-terminus by expressing chimeric topo II enzymes in which the C-terminus of one topo II isoform was exchanged for the C-terminus of the other topo II isoform. Their results revealed an absolute requirement of the C-terminal region of topo IIα (1173-1531) for in vivo association of topo II with mitotic chromosomes, which contrasts our finding demonstrating that the CTD of topo IIα spanning amino acids 1201–1454 and 1497–1531 is inhibitory for decatenation. The reason for this discrepancy could be due to truncation of the CTD at different sites, intrinsic functional differences within the C-terminal regions of topo IIα and topo IIβ or due to a significant structural alteration of topo IIα or hindrance of its catalytic site by the divergent CTD of topo IIβ.

Our previous study demonstrating an important role for tyrosine 656 in topo IIβ for regulating its catalytic activity (22) led us to examine the role of this amino acid and the homologous tyrosine, Y640, in topo IIα in regulating decatenation checkpoint and drug sensitivity. Mutation of both Y640 in topo IIα and Y656 in topo IIβ decreased the enzymatic activity, regulation of the decatenation checkpoint, and sensitivity to topo II-targeted drugs. The mechanism by which these tyrosine residues control topo II activity does not involve phosphorylation at this site, since phosphorylation of Y656 was not detected in our previous study (22) and modeling studies did not predict phosphorylation at either Y640 or Y656. These findings suggest that structural features within the CTD, compared to those in the TOPRIM domain, may be more important for modulating the dynamic functional activities of topo IIα and topo IIβ.

Because of the essential role of topo II in several DNA metabolic processes, this enzyme is a key target for clinically effective drugs used for treating several types of cancers. Although it has been assumed that most of these drugs target both isoforms, recent evidence suggests that some of these drugs may target a specific topo II isoform. Indeed in this study we show that VP-16 is more specific for topo IIα, whereas *m*-AMSA is more specific for topo IIβ. The structural features within topo II that determine sensitivity to these drugs are similar to those that influence the decatenation checkpoint. Thus C-terminal deletion of topo IIα enhances sensitivity to topo IIα-targeted drugs whereas C-terminal deletion of topo IIβ decreases sensitivity to topo IIβ-targeted drugs. Mutation of Y640 in topo IIα and Y656 in topo IIβ both decrease sensitivity of cells to topo IIα- and topo IIβ-targeted drugs, respectively. These findings further strengthen the role of these structural features in topo II function.

Since the sequences of the CTD of both topo IIα and topo IIβ are predicted to be intrinsically disordered, the crystal structure of this domain is not available. However, sequence alignment analysis of the CTDs of topo IIα and topo IIβ provided potential insights regarding structural differences within this region that might contribute to the opposing regulation of the decatenation checkpoint and drug sensitivity by C-terminal deletion mutants. The presence of additional amino acids in the CTD of topo IIβ that are negatively charged and contain multiple phenylalanines, suggests that at least in topo IIβ the CTD is prone to protein-protein rather than protein-DNA interactions. The large number of predicted PTMs within the CTDs of topo IIβ, could also alter protein–protein interactions, such that the proteins recruited by topo IIβ would play an important role in its interaction with and decatenation of its DNA substrate. Thus C-del topo IIβ would not be as proficient in binding and decatenating DNA. In the case of topo IIα, which preferentially relaxes and decatenates positively supercoiled DNA (39), analysis of the crystal structure suggests that when the CTD is deleted (as shown in the coarse grain model relative to the DNA binding domain in Supplementary Figure S7) the DNA T segment freely passes through the G gate by simple diffusion. This structural configuration provides a potential explanation as to why the C-

del enzyme is more efficient and functions at a faster rate. However, the report indicating that mutation of the phosphorylation site, serine 1524, in the CTD decreases the ability of the topo IIα to control the decatenation checkpoint (18) suggests that regulation of topo IIα enzyme activity by this region may be complex and influenced by collective PTMs at several of the predicted sites.

Comparison of the crystal structure and homology modeling of topo IIα and topo IIβ within the Y640/Y656 TOPRIM regions of topo IIα and topo IIβ, respectively revealed that the DNA interaction propensity of TOPRIM in topo IIβ is increased compared to topo IIα, since (a) the T DNA in topo IIβ is located on the direction and proximity of Y656, (b) the RI and R2 regions that provide critical anchoring contacts in topo IIα are lost in topo IIβ and (c) number of basic amino acids in TOPRIM of topo IIβ are increased. These structural features could therefore allow for better interaction and alignment of the TOPRIM domain in topo IIβ with T DNA.

In summary, our study demonstrates that the functional activity of topo IIα and topo IIβ may not be as exclusive as previously projected and these two isoforms can indeed perform overlapping functions, albeit with different efficiencies. Since topo II activity is required for cell survival, the ability of the constitutive topo IIβ isoform to substitute for the cell cycle regulated topo IIα isoform would be beneficial, especially under conditions leading to altered expression of topo IIα during the cell cycle or aberrant regulation of this isoform in proliferating cells. Further, the ability of topo IIα and topo IIβ to be distinctly regulated would allow one isoform to better compensate for the functional loss of the other. Thus future studies of topo II cellular function or regulation should involve characterization of both isoforms.

SUPPLEMENTARY DATA

Supplementary Data are available at NAR Online.

FUNDING

This work was supported by Romanian Academy programs 1 & 3 of Institute of Biochemistry (MDS, MAM & AJP); and UEFISCDI grant PN-II-ID-PCE-2011-3-0342 (MDS, MAM & AJP). Funding for open access charge: Institutional funding.
Conflict of interest statement. None declared.

REFERENCES

1. Wang,J.C. (2002) Cellular roles of DNA topoisomerases: a molecular perspective. *Nature reviews. Molecular cell biology*, **3**, 430–440.
2. Kellner,U., Sehested,M., Jensen,P.B., Gieseler,F. and Rudolph,P. (2002) Culprit and victim – DNA topoisomerase II. *The Lancet. Oncology*, **3**, 235–243.
3. Watt,P.M. and Hickson,I.D. (1994) Structure and function of type II DNA topoisomerases. *The Biochemical journal*, **303**, 681–695.
4. Woessner,R.D., Mattern,M.R., Mirabelli,C.K., Johnson,R.K. and Drake,F.H. (1991) Proliferation- and cell cycle-dependent differences in expression of the 170 kilodalton and 180 kilodalton forms of topoisomerase II in NIH-3T3 cells. *Cell growth & differentiation : the molecular biology journal of the American Association for Cancer Research*, **2**, 209–214.
5. Turley,H., Comley,M., Houlbrook,S., Nozaki,N., Kikuchi,A., Hickson,I.D., Gatter,K. and Harris,A.L. (1997) The distribution and expression of the two isoforms of DNA topoisomerase II in normal and neoplastic human tissues. *British journal of cancer*, **75**, 1340–1346.
6. Aoyama,M., Grabowski,D.R., Isaacs,R.J., Krivacic,K.A., Rybicki,L.A., Bukowski,R.M., Ganapathi,M.K., Hickson,I.D. and Ganapathi,R. (1998) Altered expression and activity of topoisomerases during all-trans retinoic acid-induced differentiation of HL-60 cells. *Blood*, **92**, 2863–2870.
7. Tsutsui,K., Tsutsui,K., Sano,K., Kikuchi,A. and Tokunaga,A. (2001) Involvement of DNA topoisomerase IIbeta in neuronal differentiation. *The Journal of biological chemistry*, **276**, 5769–5778.
8. Chikamori,K., Hill,J.E., Grabowski,D.R., Zarkhin,E., Grozav,A.G., Vaziri,S.A., Wang,J., Gudkov,A.V., Rybicki,L.R., Bukowski,R.M. *et al.* (2006) Downregulation of topoisomerase IIbeta in myeloid leukemia cell lines leads to activation of apoptosis following all-trans retinoic acid-induced differentiation/growth arrest. *Leukemia*, **20**, 1809–1818.
9. Nur,E.K.A., Meiners,S., Ahmed,I., Azarova,A., Lin,C.P., Lyu,Y.L. and Liu,L.F. (2007) Role of DNA topoisomerase IIbeta in neurite outgrowth. *Brain research*, **1154**, 50–60.
10. Lyu,Y.L., Lin,C.P., Azarova,A.M., Cai,L., Wang,J.C. and Liu,L.F. (2006) Role of topoisomerase IIbeta in the expression of developmentally regulated genes. *Molecular and cellular biology*, **26**, 7929–7941.
11. Ju,B.G., Lunyak,V.V., Perissi,V., Garcia-Bassets,I., Rose,D.W., Glass,C.K. and Rosenfeld,M.G. (2006) A topoisomerase IIbeta-mediated dsDNA break required for regulated transcription. *Science (New York, N.Y.)*, **312**, 1798–1802.
12. Yang,X., Li,W., Prescott,E.D., Burden,S.J. and Wang,J.C. (2000) DNA topoisomerase IIbeta and neural development. *Science (New York, N.Y.)*, **287**, 131–134.
13. Downes,C.S., Clarke,D.J., Mullinger,A.M., Gimenez-Abian,J.F., Creighton,A.M. and Johnson,R.T. (1994) A topoisomerase II-dependent G2 cycle checkpoint in mammalian cells. *Nature*, **372**, 467–470.
14. Damelin,M. and Bestor,T.H. (2007) The decatenation checkpoint. *British journal of cancer*, **96**, 201–205.
15. Kaufmann,W.K. (2006) Dangerous entanglements. *Trends Mol Med*, **12**, 235–237.
16. Nakagawa,T., Hayashita,Y., Maeno,K., Masuda,A., Sugito,N., Osada,H., Yanagisawa,K., Ebi,H., Shimokata,K. and Takahashi,T. (2004) Identification of decatenation G2 checkpoint impairment independently of DNA damage G2 checkpoint in human lung cancer cell lines. *Cancer research*, **64**, 4826–4832.
17. Clarke,D.J., Vas,A.C., Andrews,C.A., Diaz-Martinez,L.A. and Gimenez-Abian,J.F. (2006) Topoisomerase II checkpoints: universal mechanisms that regulate mitosis. *Cell cycle (Georgetown, Tex.)*, **5**, 1925–1928.
18. Luo,K., Yuan,J., Chen,J. and Lou,Z. (2009) Topoisomerase IIalpha controls the decatenation checkpoint. *Nature cell biology*, **11**, 204–210.
19. Bower,J.J., Karaca,G.F., Zhou,Y., Simpson,D.A., Cordeiro-Stone,M. and Kaufmann,W.K. (2010) Topoisomerase IIalpha maintains genomic stability through decatenation G(2) checkpoint signaling. *Oncogene*, **29**, 4787–4799.
20. Chen,T., Sun,Y., Ji,P., Kopetz,S. and Zhang,W. (2015) Topoisomerase IIalpha in chromosome instability and personalized cancer therapy. *Oncogene*, **34**, 4019–4031.
21. Vos,S.M., Tretter,E.M., Schmidt,B.H. and Berger,J.M. (2011) All tangled up: how cells direct, manage and exploit topoisomerase function. *Nature reviews. Molecular cell biology*, **12**, 827–841.
22. Grozav,A.G., Willard,B.B., Kozuki,T., Chikamori,K., Micluta,M.A., Petrescu,A.J., Kinter,M., Ganapathi,R. and Ganapathi,M.K. (2011) Tyrosine 656 in topoisomerase IIbeta is important for the catalytic activity of the enzyme: Identification based on artifactual +80-Da modification at this site. *Proteomics*, **11**, 829–842.
23. Chikamori,K., Grabowski,D.R., Kinter,M., Willard,B.B., Yadav,S., Aebersold,R.H., Bukowski,R.M., Hickson,I.D., Andersen,A.H., Ganapathi,R. *et al.* (2003) Phosphorylation of serine 1106 in the catalytic domain of topoisomerase II alpha regulates enzymatic activity and drug sensitivity. *The Journal of biological chemistry*, **278**, 12696–12702.

24. Mirski,S.E., Gerlach,J.K. and Cole,S.P. (1999) Sequence determinants of nuclear localization in the alpha and beta subunits of human topoisomerase II. *Exp. Cell Res.* **251**, 329–339.
25. Carpenter,A.J. and Porter,A.C. (2004) Construction, characterization, and complementation of a conditional-lethal DNA topoisomerase IIalpha mutant human cell line. *Molecular biology of the cell*, **15**, 5700–5711.
26. Herzog,C.E., Holmes,K.A., Tuschong,L.M., Ganapathi,R. and Zwelling,L.A. (1998) Absence of topoisomerase IIbeta in an amsacrine-resistant human leukemia cell line with mutaant topoisomerase IIalpha. *Cancer research*, **58**, 5298–5300.
27. Linka,R.M., Porter,A.C., Volkov,A., Mielke,C., Boege,F. and Christensen,M.O. (2007) C-terminal regions of topoisomerase IIalpha and IIbeta determine isoform-specific functioning of the enzymes in vivo. *Nucleic acids research*, **35**, 3810–3822.
28. Errington,F., Willmore,E., Tilby,M.J., Li,L., Li,G., Li,W., Baguley,B.C. and Austin,C.A. (1999) Murine transgenic cells lacking DNA topoisomerase IIbeta are resistant to acridines and mitoxantrone: analysis of cytotoxicity and cleavable complex formation. *Molecular pharmacology*, **56**, 1309–1316.
29. Damelin,M., Sun,Y.E., Sodja,V.B. and Bestor,T.H. (2005) Decatenation checkpoint deficiency in stem and progenitor cells. *Cancer cell*, **8**, 479–484.
30. Wendorff,T.J., Schmidt,B.H., Heslop,P., Austin,C.A. and Berger,J.M. (2012) The structure of DNA-bound human topoisomerase II alpha: conformational mechanisms for coordinating inter-subunit interactions with DNA cleavage. *Journal of molecular biology*, **424**, 109–124.
31. Wu,C.C., Li,T.K., Farh,L., Lin,L.Y., Lin,T.S., Yu,Y.J., Yen,T.J., Chiang,C.W. and Chan,N.L. (2011) Structural basis of type II topoisomerase inhibition by the anticancer drug etoposide. *Science (New York, N.Y.)*, **333**, 459–462.
32. Wu,C.C., Li,Y.C., Wang,Y.R., Li,T.K. and Chan,N.L. (2013) On the structural basis and design guidelines for type II topoisomerase-targeting anticancer drugs. *Nucleic acids research*, **41**, 10630–10640.
33. Zhang,Y.H., Shetty,K., Surleac,M.D., Petrescu,A.J. and Schatz,D.G. (2015) Mapping and Quantitation of the Interaction between the Recombination Activating Gene Proteins RAG1 and RAG2. *The Journal of biological chemistry*, **290**, 11802–11817.
34. Marin,M.B., Ghenea,S., Spiridon,L.N., Chiritoiu,G.N., Petrescu,A.J. and Petrescu,S.M. (2012) Tyrosinase degradation is prevented when EDEM1 lacks the intrinsically disordered region. *PloS one*, **7**, e42998.
35. Sathyapriya,R., Vijayabaskar,M.S. and Vishveshwara,S. (2008) Insights into protein-DNA interactions through structure network analysis. *PLoS computational biology*, **4**, e1000170.
36. Hendriks,I.A., D'Souza,R.C., Yang,B., Verlaan-de Vries,M., Mann,M. and Vertegaal,A.C. (2014) Uncovering global SUMOylation signaling networks in a site-specific manner. *Nat Struct Mol Biol*, **21**, 927–936.
37. Kim,W., Bennett,E.J., Huttlin,E.L., Guo,A., Li,J., Possemato,A., Sowa,M.E., Rad,R., Rush,J., Comb,M.J. *et al.* (2011) Systematic and quantitative assessment of the ubiquitin-modified proteome. *Mol Cell*, **44**, 325–340.
38. Bian,Y., Song,C., Cheng,K., Dong,M., Wang,F., Huang,J., Sun,D., Wang,L., Ye,M. and Zou,H. (2014) An enzyme assisted RP-RPLC approach for in-depth analysis of human liver phosphoproteome. *J Proteomics*, **96**, 253–262.
39. McClendon,A.K., Gentry,A.C., Dickey,J.S., Brinch,M., Bendsen,S., Andersen,A.H. and Osheroff,N. (2008) Bimodal recognition of DNA geometry by human topoisomerase II alpha: preferential relaxation of positively supercoiled DNA requires elements in the C-terminal domain. *Biochemistry*, **47**, 13169–13178.
40. Papillon,J., Menetret,J.F., Batisse,C., Helye,R., Schultz,P., Potier,N. and Lamour,V. (2013) Structural insight into negative DNA supercoiling by DNA gyrase, a bacterial type 2A DNA topoisomerase. *Nucleic acids research*, **41**, 7815–7827.
41. Sakaguchi,A. and Kikuchi,A. (2004) Functional compatibility between isoform alpha and beta of type II DNA topoisomerase. *Journal of cell science*, **117**, 1047–1054.
42. Tiwari,V.K., Burger,L., Nikoletopoulou,V., Deogracias,R., Thakurela,S., Wirbelauer,C., Kaut,J., Terranova,R., Hoerner,L., Mielke,C. *et al.* (2012) Target genes of Topoisomerase IIbeta regulate neuronal survival and are defined by their chromatin state. *Proceedings of the National Academy of Sciences of the United States of America*, **109**, E934–943.
43. Zhang,Y.L., Yu,C., Ji,S.Y., Li,X.M., Zhang,Y.P., Zhang,D., Zhou,D. and Fan,H.Y. (2013) TOP2beta is essential for ovarian follicles that are hypersensitive to chemotherapeutic drugs. *Molecular endocrinology (Baltimore, Md.)*, **27**, 1678–1691.
44. Xiao,H., Mao,Y., Desai,S.D., Zhou,N., Ting,C.Y., Hwang,J. and Liu,L.F. (2003) The topoisomerase IIbeta circular clamp arrests transcription and signals a 26S proteasome pathway. *Proceedings of the National Academy of Sciences of the United States of America*, **100**, 3239–3244.
45. Isik,S., Sano,K., Tsutsui,K., Seki,M., Enomoto,T., Saitoh,H. and Tsutsui,K. (2003) The SUMO pathway is required for selective degradation of DNA topoisomerase IIbeta induced by a catalytic inhibitor ICRF-193(1). *FEBS letters*, **546**, 374–378.
46. Dickey,J.S. and Osheroff,N. (2005) Impact of the C-terminal domain of topoisomerase IIalpha on the DNA cleavage activity of the human enzyme. *Biochemistry*, **44**, 11546–11554.
47. Lavrukhin,O.V., Fortune,J.M., Wood,T.G., Burbank,D.E., Van Etten,J.L., Osheroff,N. and Lloyd,R.S. (2000) Topoisomerase II from Chlorella virus PBCV-1. Characterization of the smallest known type II topoisomerase. *The Journal of biological chemistry*, **275**, 6915–6921.
48. Meczes,E.L., Gilroy,K.L., West,K.L. and Austin,C.A. (2008) The impact of the human DNA topoisomerase II C-terminal domain on activity. *PloS one*, **3**, e1754.